Neuro-Oncology
23(10), 1789–1797, 2021 | doi:10.1093/neuonc/noab057 | Advance Access date 10 March 2021

MR-guided focused ultrasound liquid biopsy enriches circulating biomarkers in patients with brain tumors

Ying Meng, Christopher B. Pople, Suganth Suppiah, Maheleth Llinas, Yuexi Huang, Arjun Sahgal, James Perry, Julia Keith, Benjamin Davidson, Clement Hamani, Yutaka Amemiya, Arun Seth, Hon Leong, Chinthaka C. Heyn, Isabelle Aubert, Kullervo Hynynen, and Nir Lipsman

Sunnybrook Research Institute, Toronto, Ontario, Canada (Y.M., C.B.P., M.L., Y.H., A.Sahgal, J.P., J.K., B.D., C.H., Y.A., A.Seth, H.L., C.C.H., I.A., K.H., N.L.); Division of Neurosurgery, Department of Surgery, University of Toronto, Toronto, Ontario, Canada (Y.M., S.S., B.D., C.H., N.L.); Odette Cancer Centre, Sunnybrook Health Sciences Centre, Toronto, Ontario, Canada (A.Sahgal, J.P.); Department of Radiation Oncology, Faculty of Medicine, University of Toronto, Toronto, Ontario, Canada (A.Sahgal); Division of Neurology, Department of Medicine, University of Toronto, Toronto, Ontario, Canada (J.P.); Department of Laboratory Medicine and Pathobiology, University of Toronto, Toronto, Ontario, Canada (J.K., A.Seth, I.A.); Department of Medical Imaging, Sunnybrook Health Sciences Centre, University of Toronto, Toronto, Ontario, Canada (C.C.H.); Department of Medical Biophysics, University of Toronto, Toronto, Ontario, Canada (H.L., K.H.)

Corresponding Author: Nir Lipsman, MD, PhD, Division of Neurosurgery, Harquail Centre for Neuromodulation, Hurvitz Brain Sciences Research Program, Sunnybrook Health Sciences Centre, Sunnybrook Research Institute, 2075 Bayview Avenue, Toronto, Ontario, Canada M4N 3M5 (nir.lipsman@sunnybrook.ca).

Abstract

Background. Liquid biopsy is promising for early detection, monitoring of response, and recurrence of cancer. The blood-brain barrier (BBB) limits the shedding of biomarker, such as cell-free DNA (cfDNA), into the blood from brain tumors, and their detection by conventional assays. Transcranial MR-guided focused ultrasound (MRgFUS) can safely and transiently open the BBB, providing an opportunity for less-invasive access to brain pathology. We hypothesized that MRgFUS can enrich the signal of circulating brain-derived biomarkers to aid in liquid biopsy.

Methods. Nine patients were treated in a prospective single-arm, open-label trial to investigate serial MRgFUS and adjuvant temozolomide combination in patients with glioblastoma (NCT03616860). Blood samples were collected as an exploratory measure within the hours before and after sonication, with control samples from non-brain tumor patients undergoing BBB opening (BBBO) alone (NCT03739905).

Results. Brain regions averaging 7.8 ± 6.0 cm^3 (range 0.8-23.1 cm^3) were successfully treated within 111 ± 39 minutes without any serious adverse events. We found MRgFUS acutely enhanced plasma cfDNA (2.6 ± 1.2-fold, $P < .01$, Wilcoxon signed-rank test), neuron-derived extracellular vesicles (3.2 ± 1.9-fold, $P < .01$), and brain-specific protein S100b (1.4 ± 0.2-fold, $P < .01$). Further comparison of the cfDNA methylation profiles suggests a signature that is disease- and post-BBBO-specific, in keeping with our hypothesis. We also found cfDNA-mutant copies of isocitrate dehydrogenase 1 (IDH1) increased, although this was in only one patient known to harbor the tumor mutation.

Conclusions. This first-in-human proof-of-concept study shows MRgFUS enriches the signal of circulating brain-derived biomarkers, demonstrating the potential of the technology to support liquid biopsy for the brain.

Key Points

- MRgFUS can noninvasively open the BBB, which limits therapeutic access and the liquid biopsy of brain pathologies.
- In patients with GBM, we showed that MRgFUS enhances circulating brain-derived biomarkers, supporting the feasibility of MRgFUS to aid liquid biopsy.

Importance of the Study

The BBB limits therapeutic access to the brain as well as the detection of brain pathology peripherally through liquid biopsy. Some rodent studies have shown that FUS-induced opening of the BBB releases intraparenchymal substances, such as brain-specific proteins and mRNA. We report first-in-human proof-of-concept data showing MRgFUS opening of the BBB in glioblastoma patients enhanced circulating brain-derived proteins, neuron-derived extracellular vesicles, and cell-free DNA. Further differential analysis suggests the cell-free DNA is brain-derived and disease-specific, providing data for the feasibility of a focused ultrasound framework to liquid biopsy in neuro-oncology patients.

Liquid biopsy involves the detection and analysis of pathology-derived material in blood without the need for invasive interventions such as open surgery. In cancer, it has the potential to provide a unifying platform for diagnosis, inform treatment selection by detecting resistant or sensitive tumor variants, and support disease response monitoring.[1–4] This approach has made tremendous strides in systemic cancers, with the development of several clinically approved assays for circulating tumor DNA (ctDNA) and circulating tumor cells, among others. Its use for central nervous system (CNS) tumors, however, is limited by the blood-brain barrier (BBB), which prevents biomarker shedding.[5] Even with the altered blood-tumor barrier, there is substantial heterogeneity in permeability that would prevent representation of the tumor in circulation.[6] Therefore, the sensitive detection of brain-derived biomarkers reflecting the pathology, such as rare ctDNA amongst the circulating cell-free DNA (cfDNA), is a major goal of the field to achieve applications in the clinic.

Low-intensity MR-guided focused ultrasound (MRgFUS) is an emerging technology that permits noninvasive access to brain pathology by inducing transient BBB opening (BBBO).[7] MRI guidance imparts spatially precise and flexible selection of sonicated brain regions. Early phase clinical trials have demonstrated safety and feasibility in patients' neuro-oncology and neurodegenerative disorders.[8–12] So far, the technology has been mainly utilized for drug delivery by increasing the BBB permeability to complex biological therapeutics such as antibodies and immune cells.[13,14] However, animal experiments show that the same mechanical BBBO can allow the release of intraparenchymal substances.[15,16] Here, we report a first-in-human study demonstrating that noninvasive, transient opening of the BBB using MRgFUS technology can enrich circulating brain-derived biomarkers with potential applications in liquid biopsy.

Materials and Methods

Study Design

The prospective single-arm, open-label trial was designed to investigate the safety and feasibility of serial MRgFUS and adjuvant temozolomide combination in patients with WHO grade IV glioblastoma (GBM). Details of the inclusion and exclusion criteria can be found in Supplementary Table S1. Blood samples were collected from all patients for exploratory analysis. Non-brain tumor control samples were provided by the initial patients enrolled in the MRgFUS BBBO for Alzheimer's disease (AD) study. Both trials were conducted with the approval of Sunnybrook Health Sciences Centre Research Ethics Board, Health Canada, and registered with clinicaltrials.gov (GBM—NCT03616860, AD—NCT03739905). All participants gave written informed consent for study activities.

Cancer patients underwent the procedure on the first day of every cycle, approximately 30 minutes after ingesting oral temozolomide prescribed by the study neuro-oncologist (Figure 1A). Procedures were performed with the ExAblate Neuro hemispheric device (InSightec, Israel) coupled with GE 3-Tesla MRI. The device consists of a hemispherical dome with 1024 individual 220-kHz transducer elements that enable precise transcranial MRgFUS delivery. The procedure has been described previously.[10,11] Specifically, the treatment volumes were prescribed by the neurosurgeon by outlining any non-enhancing tumor and a 1-cm peritumoral non-enhancing margin on 4-mm interval axial MRIs (Figure 1B,C). Each contour was then filled in by the device software with sonication points separated by 2.5 mm, with approximately 7 mm out-of-plane depth (Figure 1C). Contours were kept to less than 20 spots. Ultrasound delivery was performed contour-by-contour in a serial fashion and was automated using real-time acoustic emission. In the case of control patients with AD, widespread regions including the hippocampus and parietal lobe were treated by targeting in a similar fashion. Upon completion of the procedure, patients were allowed to leave once meeting routine discharge criteria. Standard-of-care procedures (eg, MRI) and RANO assessments continued as usual. The procedures ended for a patient (ie, study exit) when adjuvant temozolomide was no longer indicated (eg, progressive disease or drug toxicity).

T1-Weighted MRI Analysis

BBBO was assessed by contrast-enhanced T1-weighted MRIs, which have been validated against histological markers of BBB integrity.[17,18] Intensity difference maps were calculated from same and next day scans by brain extraction, rigid-body co-registration, masking to the region

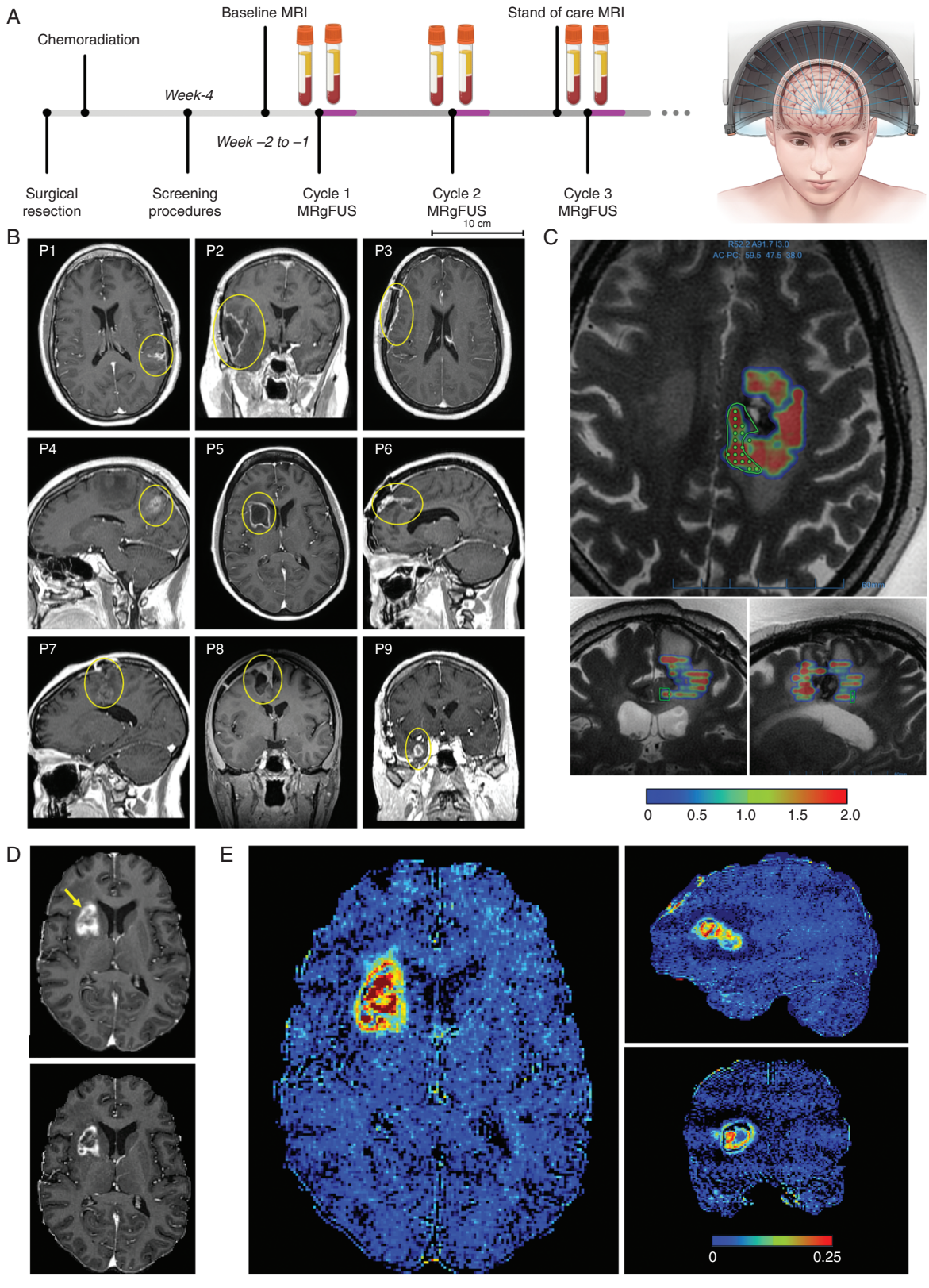

Fig. 1 Opening of the blood-brain barrier in large brain regions is achieved with transcranial MR-guided focused ultrasound. (A) Schematic diagram of MRgFUS device and study design with BBBO procedures overlapping adjuvant chemotherapy regimen in patients with glioblastoma

of interest, rescaling to 0 and 1, and subtraction (FMRIB Software Library v6.0, Advanced Normalization Tools v2.1).

Blood Collection and S100b Measurement

For all patients, blood was collected immediately prior to, and following, each procedure in EDTA-coated tubes (BD, 366643). Within 30 min of collection, plasma tubes were centrifuged at 800 *g* for 10 min at 4°C, then 12 000 *g* for 10 min at room temperature. Clarified supernatant was aliquoted into DNA LoBind tubes (Eppendorf, 22431021) for storage at –80°C. Sample for any analysis will have undergone at the most one freeze-thaw cycle. S100b protein levels were measured via enzyme-linked immunosorbent assay kit (Sigma-Aldrich, EZHS100B-33K) as per the manufacturer's instructions.

cfDNA Extraction

We used MagMAX Cell-Free DNA Isolation kit (Applied Biosystems, A29319) to extract cfDNA. DNA concentration was measured by the Qubit 3.0 Fluorometer with Qubit dsDNA HS Assay Kit (Invitrogen, Q32854) and fragmentation pattern assessed using the Agilent 2100 Bioanalyzer with Agilent High Sensitive DNA Kit, following the manufacturer's instructions.

Methylation Profile Analysis

100-200 ng of extracted cfDNA, which was necessarily pooled for pre-BBBO samples, were bisulfite-converted using EZ DNA Methylation kit (Zymo Research, D5002) following the manufacturer's protocol. Effective conversion was confirmed by qPCR amplification of converted and unconverted β-actin (Supplementary Table S2). Bisulfite-converted DNA was evaluated for methylation profiling using Illumina MethylationEPIC 850k array (Illumina, USA). Preprocessing with background subtraction adjustment was performed using GenomeStudio (Illumina, USA). Raw data files were processed using the minfi package (Bioconductor) in R and normalized. Probes that overlap with known single nucleotide polymorphisms, and probes that map to X and Y chromosomes were filtered out. Methylation values were exported as β values. For unsupervised clustering, we performed a principal component analysis on the top 100 000 most variably methylated probes based on mean absolute deviation. Furthermore, differentially methylated probes between pre- and post-BBBO samples were identified by an absolute difference of mean β value >0.1 and false discovery rate (FDR) corrected $P < .05$. Functional enrichment analysis was conducted using g:Profiler tool.

Plasma Extracellular Vesicles (EVs)

Neural cell adhesion molecule (NCAM, CD56) and L1 cell adhesion molecule (L1CAM, CD171) double positive EVs were measured by mixing and incubating 20 µL of plasma with Alexa Fluor 647 mouse anti-human CD56 (2 µL, BD Biosciences #557711) and PE mouse anti-human CD171 (2 µL, BD Biosciences #564193) at room temperature. Isotype controls were prepared similarly with Alexa Fluor 647 mouse IgG1 κ isotype control (2 µL, BD Biosciences # 57714) and PE Mouse IgG2a κ isotype control (2 µL, BD Biosciences #553457). A plasma sample from one cycle in every patient (Supplementary Table S3) was diluted by 1:30 in sterile medical-grade water and measured in duplicates using a nanoscale flow cytometer (Apogee Flow Systems Inc., A60Micro-Plus) calibrated with Apogee calibration bead mix. Data analysis was performed using Apogee Histogram Software v2020.

Droplet Digital PCR (ddPCR)

Frequency of isocitrate dehydrogenase 1 (IDH1) R132H mutations in plasma-derived cfDNA was assessed using a Bio-Rad QX200 ddPCR system. The ddPCR reaction was performed in a 20 µL volume containing 10 ng of isolated plasma cfDNA or IDH1 R132H immunopositive tumor DNA (positive control), 10 µL of ddPCR Supermix for Probes (No dUTP; Bio-Rad, cat. #186-3023) and 1 µL of Human FAM IDH1 p.R132H c.395G>A ddPCR Mutation Detection Assay (Bio-Rad, Assay ID dHsaMDV2010055). After mixing by vortexing and a spin down, droplets were generated using a QX200 Droplet Generator. Droplets were pipetted into a 96-well PCR plate, which was sealed and cfDNA samples amplified in the C1000 Touch Thermal Cycler (Bio-Rad) using the manufacturer's recommended protocol. The fluorescent signal in each droplet was read with a QX200 Droplet Reader. Mutant and wild-type droplets were quantified using QuantaSoft analysis software ver.1.7.4.0917 (Bio-Rad).

Statistical Analysis

Descriptive statistics were used to summarize results, but wherever possible all data points were presented. Pairwise data were compared using Wilcoxon signed-rank test, with an alpha of 0.05.

after surgical resection and concurrent chemoradiation. Blood samples are collected immediately before and after sonications on the same day of the procedure. (B) Representative images of the lesions (yellow circles) on baseline MRI for each patient. (C) Ultrasound can be targeted specifically to an operator-defined contour. The green polygon represents one of many target contours (others not shown). The color map indicates the cavitation dose detected by device upon ultrasound delivery. In (D), the top panel shows contrast extravasation in the areas of increased BBB permeability after MRgFUS for P5 (yellow arrow). The bottom panel shows partial restoration of the BBB integrity approximately 24 hours later, in comparison to the top panel and baseline image of the tumor in (B). (E) Intensity difference maps further show increased BBB permeability in P5 within large regions spatially distributed in the tumor and tumor margins. Heterogeneous changes in contrast extravasation are partially due to the underlying tumor. Abbreviations: BBB, blood-brain barrier; BBBO, BBB opening; MRgFUS, MR-guided focused ultrasound.

Results

Large Volume BBBO of the Tumor and Peritumoral Regions

Nine patients with GBM were enrolled in a single-arm trial investigating serial MRgFUS BBBO to enhance the delivery of adjuvant temozolomide therapy. All patients had undergone surgical resection, some gross total resection, and concurrent chemoradiation. The status of molecular markers was collected from clinical pathology at the time of surgery (Table 1). Notably, IDH1-R132H status by immunohistochemistry was wild type in all except patient 6 (P6).

The MRgFUS procedures were performed using a hemispheric array device (ExAblate, InSightec), overlapping the first day of each 5-day temozolomide course (Figure 1A,B). Each regimen was prescribed monthly. In total, 38 procedures were performed, with average of 7.8 ± 6.0 cm^3 (range 0.8-23.1 cm^3) of tissue treated within sonication time of 111 ± 39 minutes. In tailoring the target with MRI guidance, we prioritized the sonication of peri-tumor or peri-cavity regions as well as regions with fluid attenuated inversion recovery (FLAIR) hyperintensities to improve temozolomide penetration to presumably abnormal tissue (Figure 1C). Ultrasound delivery was automated based on real-time monitoring of the acoustic emissions.

Immediately following the procedure, T1-weighted MRI visualized additional areas of gadobutrol (604 Da) enhancement, indicative of successful BBBO. Decreases in the enhancement the next day in all cases demonstrate partial or complete restoration of the BBB permeability (Figure 1D). Maps of intensity differences show the spatial distribution of BBBO to envelope the tumor, which was feasible even for large, deep-seated lesions (Figure 1E). The MRgFUS treatments were overall well tolerated in all patients without any serious adverse events in keeping with previous reports (Supplementary Table S4).[8,10]

Transient BBBO Increases the Concentration of Liquid Biopsy Analytes

Blood samples were collected within 3 hours prior to the first sonication—during patient preparation—and on average 34 minutes after the last sonication. Plasma cfDNA concentration was acutely elevated after BBBO by 2.6 ± 1.2-fold (from 7.0 ± 3.3 ng/mL to 16.3 ± 5.2 ng/mL of plasma, $P < .01$, Figure 2A). Values from individual cycles are listed in Supplementary Table S5. Up to a 7-fold increase in yield was measured. The cfDNA enhancement was consistently observed longitudinally through the adjuvant temozolomide cycles (Figure 2B). To assess the quality and fragmentation pattern of the cfDNA, we performed DNA electrophoresis on one paired samples from each patient, and found the 0-280 bp fragments increased from 4.9 ± 3.9 to 17.0 ± 14.9 ng/mL of plasma ($P < .01$) (Figure 2C, Supplementary Figure S1). These mononucleosome-sized cfDNA fragments are released during apoptosis and are relatively protected from rapid degradation in circulation.[19]

MRgFUS induced cfDNA increase appeared to share a positive correlation with treated volume (Spearman's correlation 0.33, $P = .04$, Figure 2D), and a weaker negative correlation with time elapsed from sonication (Spearman's correlation 0.22, $P = .20$, Supplementary Figure S2). The level of cfDNA enhancement in two patients with subtotal resection was not different from the others (Supplementary Figure S3A), but there was a trend of greater enhancement with tumor progression (Supplementary Figure S3B).

We evaluated the possibility that a transient BBBO increases brain-derived biomarkers, specifically neuron-derived extracellular vesicles (ndEV) and S100 calcium-binding protein B (S100b). The latter is primarily expressed by astrocytes. The former is robustly and specifically marked by NCAM and L1CAM surface proteins, and provides a diagnostic platform that can dynamically reflect and track neuropathological changes in vivo.[20] From one randomly selected cycle from each patient, we observed a 3.2 ± 1.9-fold ($P < .01$, Figure 2E) increase in double-positive NCAM and L1CAM particles using nanoscale flow cytometry (Supplementary Figure S4), and a 1.4 ± 0.2-fold ($P < .01$, Figure 2F) in S100b.

Post-BBBO cfDNA Have Distinctive Disease-Specific Signature

DNA methylation profiling is a powerful tool for classification of CNS tumors and their subtypes.[21] Unsupervised clustering of methylation microarray data of pre- and

Table 1 Patient Demographics

Patient	Age	Gender	Eloquent Location	Extent of Resection	MGMT Promoter	IDH-1 R132H
P1	49	F	Yes	GTR	NA	Wild type
P2	52	M	No	GTR	Methylated	Wild type
P3	56	F	No	GTR	Unmethylated	Wild type
P4	35	M	Yes	STR	NA	Wild type
P5	56	F	Yes	STR	Unmethylated	Wild type
P6	42	F	No	GTR	NA	Mutation
P7	40	F	Yes	GTR	Unmethylated	Wild type
P8	36	F	Yes	GTR	Unmethylated	Wild type
P9	68	M	No	GTR	Methylated	Wild type

Abbreviations: GTR, gross total resection; IDH, isocitrate dehydrogenase; MGMT, O[6]-methylguanine-DNA methyltransferase; NA, not available; STR, subtotal resection.

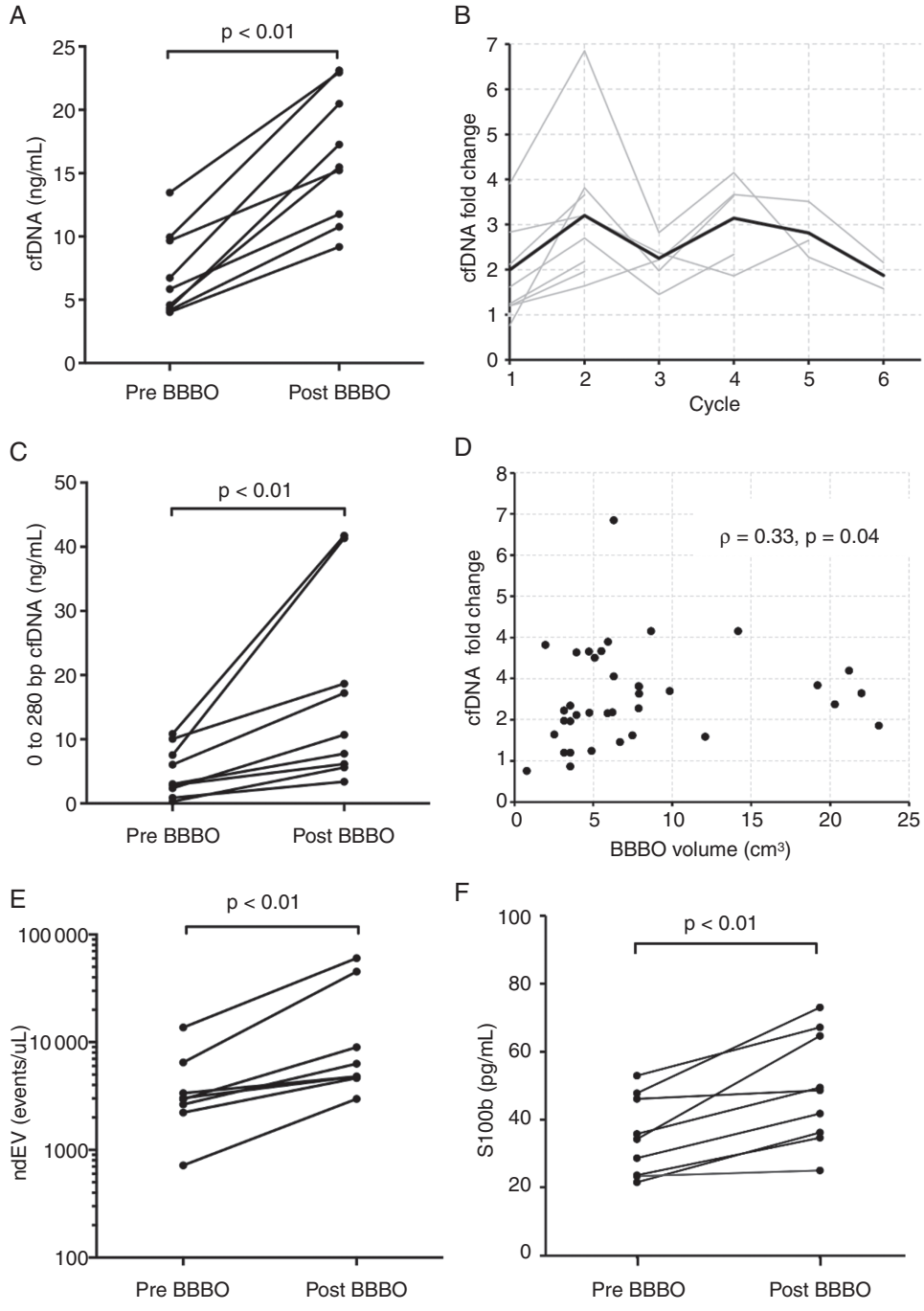

Fig. 2 Transient blood-brain barrier opening enriches signal of circulating biomarkers. (A) Plasma cfDNA concentration was significantly enhanced after noninvasive MRgFUS BBBO. Each data point represents the mean cfDNA concentration for each patient. (B) The fold change in plasma cfDNA concentration is graphed over the course of adjuvant chemotherapy. Each gray line represents a single patient. The red line indicates the group mean at each cycle. (C) The concentration of single nucleosome length cfDNA was also increased after BBBO. (D) The fold change in plasma cfDNA concentration at each cycle is plotted against the volume of BBBO, demonstrating a positive Spearman's correlation between the two variables. Each point represents the data at one cycle. (E) L1CAM and NCAM double-positive extracellular vesicles are increased after BBBO. (F) Plasma S100b levels are significantly increased after BBBO. In (C), (E), and (F), measurements were taken pre- and post-BBBO at only one cycle per patient, given the availability of samples. Abbreviations: BBBO, BBB opening; cfDNA, cell-free DNA; MRgFUS, MR-guided focused ultrasound; ndEV, neuron-derived extracellular vesicle.

post-BBBO cfDNA by principal component analysis shows a clear separation of the two groups by principal component 1, explaining for 25% of the variability (Figure 3A). It was necessary to pool pre-BBBO samples collected from multiple cycles due to low cfDNA yield, while it was feasible to perform post-BBBO analysis on single sessions. Direct

comparison of the β values found 95% (330 of 346) of the differentially methylated probes in the post-BBBO samples were hypomethylated compared to pre-BBBO, suggestive of a cancer signature (Supplementary Figure S5).

We performed a gene set enrichment analysis on the group of hypomethylated probes using g:Profiler. Based on protein expression data from the Human Protein Atlas, the set was significantly enriched for glia and neuron as well as immunologic cells (Figure 3B). Of biological processes, enriched terms consisted of immune activation, vesicle-mediated transport, regulation of cell communication, and DNA-binding transcription factor activity.

To determine whether the methylation signature of post-BBBO samples was unique to GBM patients, we incorporated control plasma samples provided by two non-brain tumor patients with a history of Alzheimer's undergoing MRgFUS BBBO alone. Principal component analysis showed a clustering suggestive of post-BBBO samples having differentiated signatures amongst patients with different neurological disorders (Figure 3C).

IDH1 mutational status is one of the most important molecular classification and prognostication factors for high-grade gliomas.[22] Only one GBM tumor out of nine was immunopositive for the R132H mutation. Targeted analysis of two different cycles with ddPCR, a highly sensitive technique, found 3.5 and 5 IDH1-R132H-mutant copies per 10-ng cfDNA, which is considered a positive readout.[23] These measurements represent a 2- to 3-fold increase from 1.6 mutant copies measured in the same input pre-BBBO cfDNA. In comparison, post-BBO samples from two patients with IDH1 wild-type tumors had 1.7 ± 0.1 mutant copies per 10 ng cfDNA.

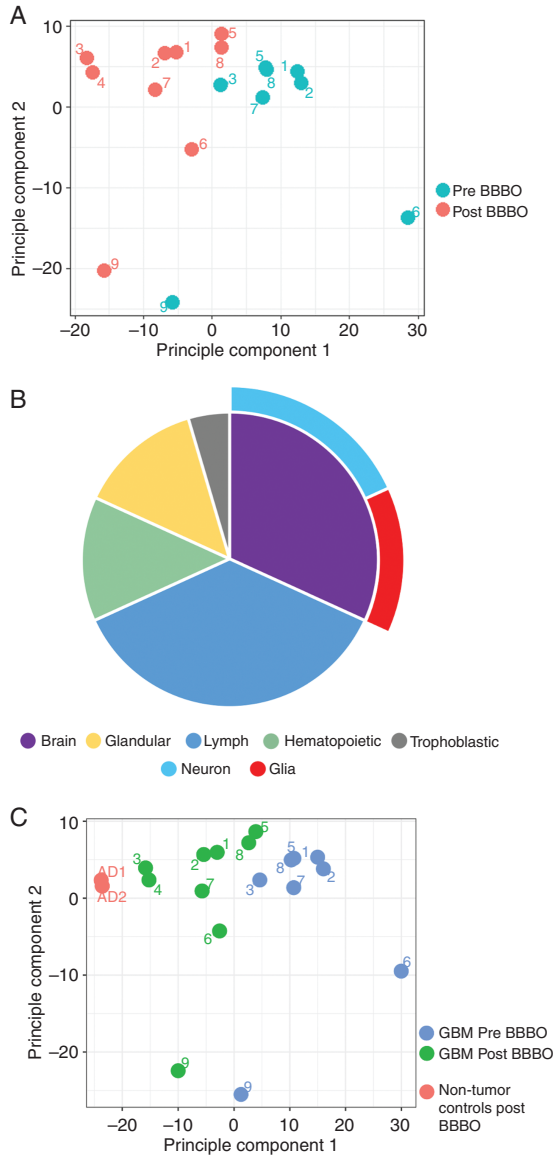

Fig. 3 Post-BBBO cfDNA has distinctive disease-specific signature. (A) Principal component analysis shows a separation of the methylation signature of pre- and post-BBBO cfDNA. (B) Results of a functional enrichment analysis of the differentially hypomethylated probe set based on the Human Protein Atlas. (C) Results of a principal component analysis of methylation data with cfDNA from non-brain tumor patients' post-BBBO as controls suggest disease-specific signatures. Abbreviations: BBBO, BBB opening, cfDNA, cell-free DNA; GBM, glioblastoma.

Discussion

The BBB physically limits the number of tumor analytes in the circulation. Successful detection of rare events is highly dependent on sufficient blood sampling and shedding of biomarkers from all areas of the tumor. We show for the first time in human patients that transcranial low-frequency MRgFUS can enrich the signal of circulating brain-derived biomarkers, specifically proteins, cfDNA, and EVs, to help overcome this limitation. Using methods that are increasingly accessible in clinical oncology, we found a significant increase in cfDNA yield post-MRgFUS BBBO that bear a disease-specific methylation signature unique to brain tumor patients after BBBO. The level of cfDNA enhancement might also correlate with BBBO volume and tumor progression. We also saw an increased signal in clinically actionable plasma IDH1-R132H-mutant copies, although this was in a single patient harboring the IDH1-R132H tumor mutation. Finally, we demonstrated the practical feasibility of repeated large volume BBBO in patients over the longitudinal course of adjuvant chemotherapy, further supporting the flexibility of the technology when combined with liquid biopsy for disease monitoring.

While promising, this study has several limitations. Mainly, our findings were derived retrospectively from a small group of GBM patients, which limits statistical analysis and validation. In particular, the targeted detection of IDH1-R132H ctDNA fell on the one patient with this specific mutation. Given the broad array of analytes explored, later experiments such as the ddPCR were limited by the biological sample remaining available. Furthermore, the low numbers and inconsistent availability of tissue samples restricted a coordinated effort at molecular characterization.

Indeed, the primary objective of this phase I trial was to investigate the safety of MRgFUS BBBO after surgical resection and chemoradiation. As such, the sonication tissue likely contained a mixture of inflammatory, tumor, and necrotic cells, which might be deduced by the functional enrichment of analysis of the differentially methylated promoters. A general sonication effect also cannot be entirely excluded. Therefore, the effect of BBBO on circulating tumor cells and mutant DNA copies, as well as the rate of false-positive or -negative in FUS aided liquid biopsy results when compared against gold standard neuropathology examinations will be interrogated in future studies with control or validation groups. Also, fundamental issues, such as the optimal interval for blood collection, which might depend on the temporal dynamics of the BBBO and analyte of interest, are important areas for future investigation. More specifically, serial blood sampling post sonications, at both minute and hour timeframes, will help better characterize the kinetics of biomarker changes post-BBBO. To minimize the burden on patients, we did not perform serial phlebotomies in this pilot group.

Nevertheless, our findings represent a novel, first-in-human data that is hypothesis-generating for a valuable application of MRgFUS in medicine. They set the stage for investigations in MRgFUS-based liquid biopsy of brain tumors and other brain pathologies as the sole objective or simultaneously with drug delivery for optimized, personalized medicine. For instance, MRgFUS could combine with standard-of-care adjuvant temozolomide to enhance delivery, and at the same time help assay changes in tumor microenvironment that might predict recurrence or a need for alternative therapy prior to neuroimaging (Figure 4). This approach could also be helpful in differentiating radiation necrosis from tumor recurrence or diagnosing lesions where surgical biopsy is risky or surgical debulking is unnecessary. We found here that MRgFUS can quickly and precisely achieve BBBO repeatedly in large tumor and peritumoral volumes. This capability could facilitate a more selective or comprehensive representation of the tumor in plasma. Finally, while an advantage of signal enrichment with MRgFUS is to leverage widely available commercialized methods, it could also be combined with more complex techniques such as BEAMing (beads, emulsions, amplification, and magnetics) to improve further sensitivity.

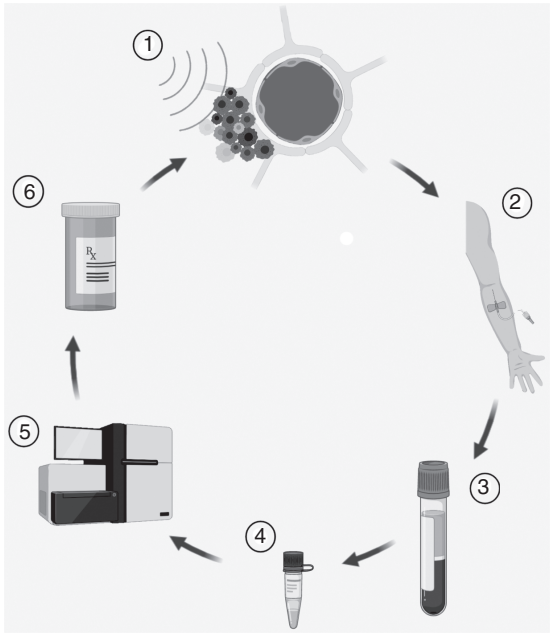

Fig. 4 A MRgFUS-based platform for both enhanced drug delivery and liquid biopsy. Concept diagram of a MRgFUS-based platform for both enhancing drug delivery and liquid biopsy to deliver personalized medicine for patients with brain tumors. MRgFUS can be combined with repeated doses of anti-tumor therapy (1), each time providing an opportunity to collect blood samples containing analytes derived from the pathology in the sonicated areas (2). After preprocessing (3) and extraction for specific markers (4), commercially available techniques (5, eg, droplet digital PCR). Biological changes in the pathology might inform a change in anti-tumor therapy (6). Abbreviation: MRgFUS, MR-guided focused ultrasound.

Supplementary Material

Supplementary material is available at *Neuro-Oncology* online.

Keywords

blood-brain barrier | brain tumor | focused ultrasound | glioblastoma | liquid biopsy

Funding

This study was investigator-initiated but funded by InSightec and supported by the Harquail Centre for Neuromodulation, as well as the Focused Ultrasound Foundation and Sunnybrook Health Sciences AFP Innovation Fund.

Acknowledgments

We acknowledge Ruby Endre and Garry Detzler for their technical assistance in this study, Dr Stanley Liu for his work on the ddPCR platform, and Hang Yu Lin for her artwork. Y.M. has been supported by the Focused Ultrasound Foundation, the Hold'em for Life Foundation, NSERC, and the PSI Foundation. H.L. is supported by a Canadian Foundation for Innovation John R. Evans Leaders Fund Grant (#39243). I.A. holds a Canada Research Chair in Brain Repair and Regeneration, Tier 1.

Conflict of interest statement. N.L. has received honorarium for serving on an expert steering committee for Focused Ultrasound Foundation, as well as research support from Focused Ultrasound Foundation and InSightec. K.H. is an inventor of intellectual property related to the brain application of focused ultrasound owned by Brigham and Women's Hospital and Sunnybrook Research Institute. Other authors do not have potential conflicts to disclose.

Author contributions. Y.M., K.H., and N.L. conceived and designed the MRgFUS study. Y.M., C.B.P., M.L., Y.H., A.Sahgal, J.P., J.K., B.D., C.H., C.C.H., K.H., and N.L. carried out the MRgFUS experiments. Y.M., C.B.P., S.S., H.L., I.A., K.H., and N.L. conceived various aspects of the biological analysis. Y.M., C.B.P., S.S., Y.A., and H.L. conducted the biological sample measurements and analysis. Y.M. and C.B.P. analyzed the neuroimaging data. All authors contributed to the interpretation of overall results. Y.M. and N.L. wrote the initial manuscript with critical input from all authors.

Data and materials availability. Data will be made available upon reasonable request to the corresponding author N.L.

References

1. Dawson SJ, Tsui DW, Murtaza M, et al. Analysis of circulating tumor DNA to monitor metastatic breast cancer. *N Engl J Med.* 2013;368(13):1199–1209.
2. Maheswaran S, Sequist LV, Nagrath S, et al. Detection of mutations in EGFR in circulating lung-cancer cells. *N Engl J Med.* 2008;359(4):366–377.
3. Shen SY, Singhania R, Fehringer G, et al. Sensitive tumour detection and classification using plasma cell-free DNA methylomes. *Nature.* 2018;563(7732):579–583.
4. Detection of glioma and prognostic subtypes by non-invasive circulating cell-free DNA methylation markers | bioRxiv. https://www.biorxiv.org/content/10.1101/601245v1. Accessed April 29, 2020
5. Cescon DW, Bratman SV, Chan SM, Siu LL. Circulating tumor DNA and liquid biopsy in oncology. *Nature Cancer.* 2020;1(3):276–290.
6. Arvanitis CD, Ferraro GB, Jain RK. The blood-brain barrier and blood-tumour barrier in brain tumours and metastases. *Nat Rev Cancer.* 2020;20(1):26–41.
7. Meng Y, Hynynen K, Lipsman N. Applications of focused ultrasound in the brain: from thermoablation to drug delivery. *Nat Rev Neurol.* 2021;17(1):7–22.
8. Carpentier A, Canney M, Vignot A, et al. Clinical trial of blood-brain barrier disruption by pulsed ultrasound. *Sci Transl Med.* 2016;8(343):343re2.
9. Idbaih A, Canney M, Belin L, et al. Safety and feasibility of repeated and transient blood-brain barrier disruption by pulsed ultrasound in patients with recurrent glioblastoma. *Clin Cancer Res.* 2019;25(13):3793–3801.
10. Mainprize T, Lipsman N, Huang Y, et al. Blood-brain barrier opening in primary brain tumors with non-invasive MR-guided focused ultrasound: a clinical safety and feasibility study. *Sci Rep.* 2019;9(1):321.
11. Lipsman N, Meng Y, Bethune AJ, et al. Blood-brain barrier opening in Alzheimer's disease using MR-guided focused ultrasound. *Nat Commun.* 2018;9(1):2336.
12. Abrahao A, Meng Y, Llinas M, et al. First-in-human trial of blood-brain barrier opening in amyotrophic lateral sclerosis using MR-guided focused ultrasound. *Nat Commun.* 2019;10(1):4373.
13. Kinoshita M, McDannold N, Jolesz FA, Hynynen K. Noninvasive localized delivery of Herceptin to the mouse brain by MRI-guided focused ultrasound-induced blood-brain barrier disruption. *Proc Natl Acad Sci U S A.* 2006;103(31):11719–11723.
14. Alkins R, Burgess A, Kerbel R, Wels WS, Hynynen K. Early treatment of HER2-amplified brain tumors with targeted NK-92 cells and focused ultrasound improves survival. *Neuro Oncol.* 2016;18(7):974–981.
15. Zhu L, Cheng G, Ye D, et al. Focused ultrasound-enabled brain tumor liquid biopsy. *Sci Rep.* 2018;8(1):6553.
16. Pacia CP, Zhu L, Yang Y, et al. Feasibility and safety of focused ultrasound-enabled liquid biopsy in the brain of a porcine model. *Sci Rep.* 2020;10(1):7449.
17. Hynynen K, McDannold N, Sheikov NA, Jolesz FA, Vykhodtseva N. Local and reversible blood-brain barrier disruption by noninvasive focused ultrasound at frequencies suitable for trans-skull sonications. *Neuroimage.* 2005;24(1):12–20.
18. McDannold N, Vykhodtseva N, Hynynen K. Use of ultrasound pulses combined with definity for targeted blood-brain barrier disruption: a feasibility study. *Ultrasound Med Biol.* 2007;33(4):584–590.
19. Sanchez C, Snyder MW, Tanos R, Shendure J, Thierry AR. New insights into structural features and optimal detection of circulating tumor DNA determined by single-strand DNA analysis. *NPJ Genom Med.* 2018;3:31.
20. Mustapic M, Eitan E, Werner JK Jr, et al. Plasma extracellular vesicles enriched for neuronal origin: a potential window into brain pathologic processes. *Front Neurosci.* 2017;11:278.
21. Capper D, Jones DTW, Sill M, et al. DNA methylation-based classification of central nervous system tumours. *Nature.* 2018;555(7697):469–474.
22. Tateishi K, Wakimoto H, Cahill DP. IDH1 mutation and World Health Organization 2016 diagnostic criteria for adult diffuse gliomas: advances in surgical strategy. *Neurosurgery.* 2017;64(CN_suppl_1):134–138.
23. Gutteridge A, Rathbone VM, Gibbons R, et al. Digital PCR analysis of circulating tumor DNA: a biomarker for chondrosarcoma diagnosis, prognostication, and residual disease detection. *Cancer Med.* 2017;6(10):2194–2202.